JOURNAL OF SOLID STATE CHEMISTRY **78**, 35–45 (1989)

Preparation and Characterization of New Mixed Sandwiched Layered Compounds $Ln_{32}Nb_{28}S_{88}$ (Ln = La, Ce)

A. MEERSCHAUT,* P. RABU, AND J. ROUXEL

Laboratoire de Chimie des Solides, UA 279, Institut de Physique et Chimie des Matériaux, 2, rue de la Houssinière, 44072 Nantes Cedex 03, France

Received June 29, 1988

New ternary $Ln_{32}Nb_{28}S_{88}$ (Ln = La, Ce) compounds have been obtained. They crystallize in the orthorhombic space group *Ccca* with a = 23.031(9) Å, b = 23.216(6) Å, c = 5.806(2) Å, and a = 22.877(9) Å, b = 23.127(13) Å, c = 5.775(2) Å for $La_{32}Nb_{28}S_{88}$ and $Ce_{32}Nb_{28}S_{88}$, respectively. The structure of $La_{32}Nb_{28}S_{88}$ (Z = 1) has been refined until R = 0.155 for 639 reflections with $I \geq 4\sigma I$ and 56 variables. The structure may be described as a mixed sandwiched layered type where $|NbS_2|$ and $|LaS|$ slabs alternate. These new compounds may be classified as misfit layer compounds.

Introduction

The chemistry of chalcogen-rich niobium and tantalum chalcogenides has led to many low-dimensional compounds among which the trichalcogenides, such as $NbSe_3$ (*1*) or NbS_3 (*2*), and the tetrachalcogenides (*3*) have shown very striking electrical properties associated with charge density wave instabilities (*4*). These compounds are built up from a metallic chain running inside a chalcogen framework which is respectively trigonal prismatic or rectangular antiprismatic. Systems involving a third element (e.g., first row transition or rare-earth metals) were recently investigated. They showed that the low-dimensional character is generally preserved, this being achieved in different ways. For instance, with 3d transition metal elements the low-dimensional character is retained either in M_xNbS_2 phases in which the M atoms are ordered between NbS_2 slabs or in phases such as $FeNb_3Se_{10}$ (*5*), Ta_2NiX_5 (X = S, Se) (*6*), or Ta_2MSe_7 (M = Ni, Pt) (*7*) in which the association of different chains is realized with each element exhibiting its preferential coordination.

The ternary systems Ln–MX_n (Ln = lanthanides) have been investigated very little. Some intercalated compounds Ln_xNbS_2 were synthesized through rare-earth solutions in liquid ammonia (*8, 9*). Ln_xTaS_2 compounds were also recently reported (*10*); they were prepared by reaction of the elements or by direct intercalation of Ln into TaS_2 powder. All these compounds exhibit a layered structural type. Donohue (*11*) reported, a long time ago, some new compounds of general formulation $LnMX_3$ (with Ln = all rare earths or Bi; M = Nb, Ta; X = S, Se). Such a series of compounds could be structurally related to already existing (Sn/Pb)–MX_3 compounds (*12, 13*).

---

* To whom all correspondence should be addressed.

0022-4596/89 $3.00

However, little information about structures or stoichiometry were given at that time. Due to its important size, a rare-earth cation may act as a structuring agent and force the Nb cations to segregate in layers. Indeed two-dimensional arrangements are already known in the chemistry of rare-earth elements and particularly in the case of *Ln*–U–O–S systems (*14, 15*). These considerations strongly favored the extension to rare earths of our investigations on new lamellar compounds. In this paper, we report new phases observed in the La–Nb–S and Ce–Nb–S systems.

TABLE I

CHEMICAL ANALYSIS: CORRECTION WEIGHT FRACTION PERCENTAGE (AVERAGE OF THREE SAMPLES)

"$LaNbS_3$"	La	Nb	S
– exp.	42.6	24.2	33.2
$LaNbS_3$ → theor.	42.35	28.32	29.33
$La_{32}Nb_{28}S_{88}$ → theor.	45.05	26.36	28.58
"$CeNbS_3$"	Ce	Nb	S
– exp.	44.4	22.2	33.4
$CeNbS_3$ → theor.	42.56	28.22	29.22
$Ce_{32}Nb_{28}S_{88}$ → theor.	45.26	26.26	28.48

Experimental

The phases were prepared by heating a mixture of Ln_2S_3 and NbS_2 (or NbS_3) in a 1 : 1 ratio at a temperature of 1050°C in silica tubes sealed under vacuum. The tubes were protected by a thin carbon film deposited by cracking acetone. Niobium and rare-earth chalcogenides were handled in a glove box under nitrogen. Products were intermediately crushed and reheated for 1 week. Finally, samples were simply cooled down to room temperature, in the furnace itself (~4 hr from 1050 to 20°C).

Single crystals in the shape of platelets were obtained when using iodine as transport agent (<5 mg cm^{-3}).

Semiquantitative analysis of these crystals were carried out with an electron microprobe (TRACOR model-dispersive energy) mounted on a scanning electron microscope. Results are summarized in Table I. They indicate compositions close to $LnNbS_3$. (From structural analysis it will actually appear to be $Ln_{32}Nb_{28}S_{88}$.)

X-ray Laüe, Buerger, and Weissenberg photographs indicated the orthorhombic *mmm* Laüe symmetry. Lattice parameters were refined by least-squares treatments of the data (Tables II and III for "$LaNbS_3$" and "$CeNbS_3$," respectively). The patterns were recorded in a Guinier camera (Nonius FR 552) with $CuK\alpha_1$ radiation ($\lambda = 1.54059$ Å and silicon as internal standard).

A single crystal of "$LaNbS_3$" with dimensions $0.33 \times 0.14 \times 0.047$ mm^3 was mounted on an Enraf–Nonius CAD4 diffractometer. $MoK\alpha$ radiation ($\lambda = 0.7107$ Å) was used. Details of the data collection process are gathered in Table IV. The list of data reflections revealed the systematic absences for hkl, with $h + k = 2n + 1$, and the following ones $0kl$, $l = 2n + 1$; $h0l$, $l = 2n + 1$; and $hk0$, $h = 2n + 1$ which are indicative of the *Ccca* space group.

Lorentz, polarization, and absorption corrections were applied. The structure was solved by means of the Patterson map and subsequent Fourier-difference syntheses. All atomic positions were found by this routine procedure. Full-matrix least-squares refinement based on F and neutral atom scattering factors taking into account the anomalous dispersion were used via the "Enraf–Nonius Structure Determination Package" (*16*). In the final stage, only lanthanum atoms were refined anisotropically using 639 unique data. Three atoms, Nb4, S1, and S4, took negative isotropic temperature values. The secondary isotropic extinction was taken into consideration during the last stage of refinement ($g = 1.57 \times$

TABLE II

$La_{32}Nb_{28}S_{88}$ GUINIER PATTERN

d_{obs} (Å)	d_{calc} (Å)	h	k	l	I/I_0	d_{obs} (Å)	d_{calc} (Å)	h	k	l	I/I_0
11.54	11.52	2	0	0	25.9	2.3150	2.3154	6	0	2	90.7
5.764	5.758	4	0	0	16.8		2.3149	6	8	0	29.5
3.874	3.866	2	4	1	97.8	2.3028	2.3031	10	0	0	6.7
3.838	3.838	6	0	0	100	2.1677	2.1670	7	7	1	27.1
3.350	3.342	4	4	1	73.2	2.0534	2.0524	0	8	2	26.0
2.9058	2.9029	0	0	2	35.7	2.0446	2.0438	8	8	0	13.7
	2.9020	0	8	0	42.3	2.0218	2.0205	2	8	2	16.7
2.8802	2.8789	8	0	0	15.7	1.8128	1.8130	2	4	3	9.0
2.8564	2.8576	1	7	1	2.1		1.8126	2	12	1	8.0
2.8178	2.8149	2	0	2	24.0	1.7492	1.7492	4	4	3	7.6
	2.8141	2	8	0	25.6		1.7488	4	12	1	7.5
2.6943	2.6964	3	7	1	1.7	1.6656	1.6671	1	7	3	24.4
2.5910	2.5921	4	0	2	2.2	1.6563	1.6583	0	14	0	4.3
	2.5915	4	8	0	1.6	1.6000	1.6010	12	0	2	4.9
2.4413	2.4419	5	7	1	21.9						

Note. $a = 23.031(9)$ Å, $b = 23.216(6)$ Å, $c = 5.806(2)$ Å; orthorhombic symmetry, space group *Ccca*.

10^{-7}). The final obtained R values are $R = 0.155$ and $R_w = 0.193$ ($w = 1$). These rather high values do not mitigate the validity of the structural model, this being discussed below. In particular the Fourier-difference map showed high background values but no residual peak. Final atomic parameters are given in Table V; thermal anisotropic parameters for La1 and La2 atoms are gathered in Table VI.

TABLE III

$Ce_{32}Nb_{28}S_{88}$ GUINIER PATTERN

d_{obs} (Å)	d_{calc} (Å)	h	k	l	I[a]	d_{obs} (Å)	d_{calc} (Å)	h	k	l	I[a]
11.47	11.44	2	0	0	s	2.3025	2.3036	6	8	0	vs
5.725	5.719	4	0	0	s		2.3020	6	0	2	
3.837	3.848	2	4	1	m	2.2857	2.2877	10	0	0	m
3.811	3.813	6	0	0	vs	2.1585	2.1556	7	7	1	w
3.319	3.325	4	4	1	m	2.0352	2.0331	8	8	0	s
2.8892	2.8909	0	8	0	s	1.9054	1.9064	12	0	0	ms
	2.8876	0	0	2			1.9022	9	7	1	
2.8586	2.8597	8	0	0	ms	1.8021	1.8008	6	8	2	m
2.7993	2.8028	2	8	0	s	1.7934	1.7932	10	0	2	m
	2.7998	2	0	2		1.6611	1.6624	8	8	2	ms
2.5780	2.5800	4	8	0	ms	1.5904	1.5915	12	8	0	vw
	2.5777	4	0	2			1.5910	12	0	2	
2.4327	2.4299	5	7	1	m	1.4435	1.4438	0	0	4	w
2.3482	2.3429	8	4	1	s						

[a] Visually estimated; vs, very strong; s, strong; m, medium; w, weak; vw, very weak.

Note. $a = 22.877(9)$ Å, $b = 23.127(13)$ Å, $c = 5.775(2)$ Å; orthorhombic symmetry, space group *Ccca*.

TABLE IV

SUMMARY OF X-RAY DATA COLLECTION AND CRYSTAL STRUCTURE REFINEMENT

Radiation	Mo$K\alpha$
Monochromator	Graphite
Data collection	Nonius CAD4 diffractometer
Scan mode	ω
Angular range	2–32°
Index limits	$0 \leq h \leq 35$, $0 \leq k \leq 35$, $0 \leq l \leq 9$
Limits reciprocal space ($\sin \theta/\lambda$)	0.15–0.70
Absorption coefficient (cm^{-1})	147.9
Transmission, limits:	0.22–0.51
Number of reflections $I \geq 4\sigma I$	639
Number of variables	56
$R = \Sigma\|\|F_o\| - \|F_c\|\|/\Sigma\|F_o\|$	0.155
$R_w = [\Sigma w(\|F_o\| - \|F_c\|)^2/\Sigma w F_o^2]^{1/2}$ with $w = 1$	0.193
Extinction coefficient	1.57×10^{-7}

Description of the Structure

The projection of the crystal structure onto the (a, b) plane (Fig. 1) reveals a juxtaposition of $|NbS_2|$ and $|LaS|$ sheets perpendicularly to the a direction, in a sequence of one trigonal prismatic $|NbS_2|$ slab for one kind of $|La–S|$ ladder.

Within the $|NbS_2|$ slab, Nb atoms are surrounded by six nearest sulfur neighbors distributed at the corners of a triangular prism. All Nb atoms are trigonal-prismatically coordinated. Especially concerning Nb atoms, some generated equivalent positions led to too short Nb–Nb contacts. Indeed, for instance, Nb1 position gives rise to two sites which roughly differ only by their z elevations (z and $1/2$-z) which corresponds to $\sim 1/3\ c$ (<2 Å). The same situation is occurring for all Nb atoms. This fact led us to assume a half-occupancy of all the Nb sites. This statistical distribution of Nb atoms could be illustrated by both cases schematized on Figs. 2a and b. Thus it can be thought that a part of $|NbS_2|$ slabs built up with $|NbS_6|$ prisms is composed of Nb1 at $z = 0.58$, and a counterpart is composed of Nb1 also but at $z = 0.92$. The same explanation about Nb occupancies holds for all Nb atoms. The $|NbS_2|$ slabs are generated parallel to the (b, c) plane by $|NbS_6|$ trigonal prisms sharing S–S vertices perpendicular to their triangular basis. It results in a nearly perfect plane of Nb atoms sand-

TABLE V

POSITIONAL AND OCCUPANCY AND THERMAL ISOTROPIC PARAMETERS FOR $La_{32}Nb_{28}S_{88}$

Atom	Posit.	Occ. (%)	x	y	z	B_{eq}[a] B_{iso}
La1	16i	100	0.3246(3)	0.069 (1)	0.497 (3)	6.6(2)[a]
La2	16i	100	0.1726(2)	0.1899(3)	0.5118(7)	1.30(7)[a]
Nb1	16i	50	−0.003 (1)	0.0280(7)	0.575 (3)	1.4(3)
Nb2	16i	50	−0.003 (1)	0.0946(7)	0.076 (3)	1.9(3)
Nb3	16i	50	0.0003(8)	0.1800(8)	0.575 (3)	0.8(2)
Nb4	8g	50	0	$\frac{1}{4}$	0.075 (3)	−0.4(2)
S1	16i	100	0.0655(6)	0.1745(6)	0.249 (3)	−0.3(2)
S2	16i	100	−0.076 (1)	0.037 (2)	0.241 (8)	3.1(5)
S3	8e	100	0.426 (2)	$\frac{1}{4}$	$\frac{1}{4}$	1.6(5)
S4	16i	100	0.0656(5)	0.1071(8)	0.750 (3)	−0.5(2)
S5	16i	100	0.196 (1)	0.186(2)	0.012 (6)	3.2(5)
S6	16i	100	0.2997(8)	0.069(1)	−0.002 (8)	1.5(3)

[a] Anisotropically refined atoms are given in the form of the isotropic equivalent thermal atoms defined as: $B_{eq} = \frac{4}{3} \Sigma_i \Sigma_j \beta_{ij} \cdot a_i \cdot a_j$.

TABLE VI

THERMAL ANISOTROPIC PARAMETERS FOR La1 AND La2

	U_{11}	U_{22}	U_{33}	U_{12}	U_{13}	U_{23}
La1	0.039(3)	0.138(4)	0.074(5)	0.020(9)	0.036(5)	0.040(6)
La2	0.017(2)	0.025(2)	0.008(1)	0.001(3)	−0.007(2)	−0.001(3)

Note. The form of the anisotropic thermal parameter is: $\exp[-2\pi^2(h^2a^{*2}U_{11} + \cdots + 2hka^*b^*U_{12} + \cdots)]$.

wiched by two sulfur planes. These latter, rather corrugated, are built up from adjacent curved planes constituted by four different sulfur atoms (S1, S2, S3, S4).

The interatomic distances between Nb atoms located along the *b* axis, and which roughly differ by *b*/2 in elevation (Table VIIB), are found in the following sequence:

$$\begin{array}{ccccccccccc} & \overset{Y=0}{\downarrow} & & & & & & \overset{Y=0.25}{\downarrow} & & & \\ \mathrm{Nb1} & \xrightarrow{3.181} & \mathrm{Nb1} & \xrightarrow{3.287} & \mathrm{Nb2} & \xrightarrow{3.519} & \mathrm{Nb3} & \xrightarrow{3.330} & \mathrm{Nb4} & \xrightarrow{3.330} & \mathrm{Nb3}\ldots \\ & & Z = 0.58 & & Z = 0.08 & & Z = 0.58 & & Z = 0.08 & & \\ & & Z = 0.92 & & Z = 0.42 & & Z = 0.92 & & Z = 0.42 & & \end{array}$$

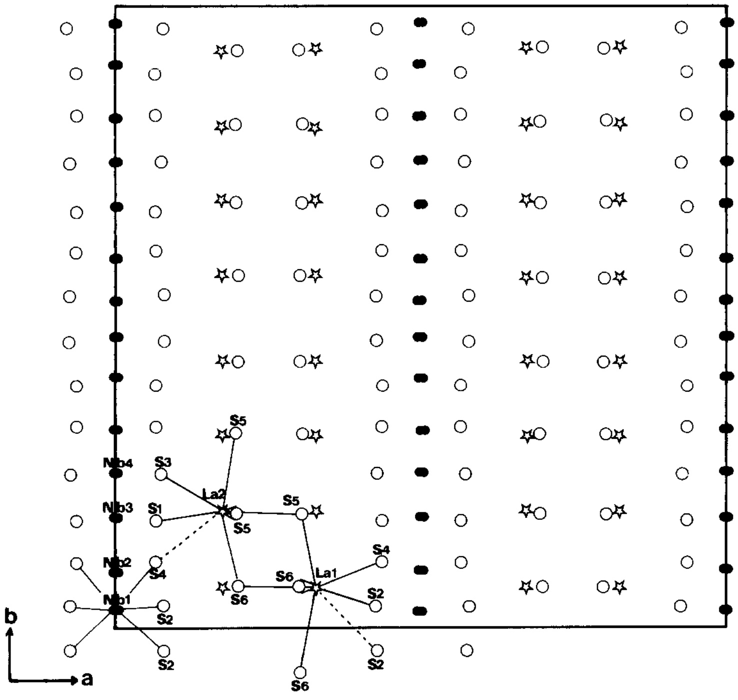

FIG. 1. Projection of the structure of $La_{32}Nb_{28}S_{88}$ onto the (*a*,*b*) plane.

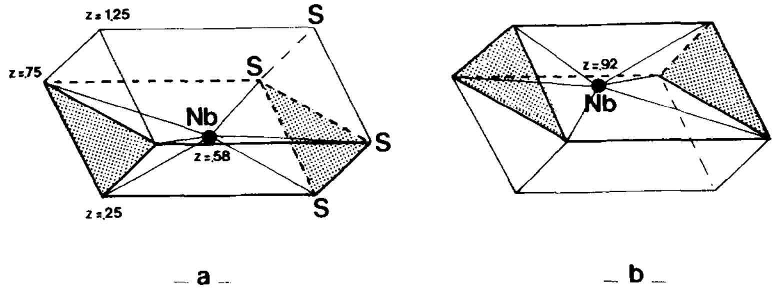

FIG. 2. Distribution of Nb atoms ($Z = 0.58$, $Z = 0.92$) in a trigonal prismatic coordination $|NbS_2|$.

Similar Nb–Nb bond values are observed for a series of pseudo-1D conductors such as the $(NbSe_4)_nI$ compounds (*3*). The interatomic Nb–S distances within the $|NbS_6|$ polyhedra are given in Table VIIA.

The |LaS| slab is made of a double row of La atoms, perpendicular to the *a* axis. The La atoms have eight closest sulfur neighbors, which can be, in fact, decomposed into 6 + 2 and 7 + 1 in the case of La1 and La2, respectively (Table VIIA). The average La–S distances (3.04 Å for La1 and 3.01 Å for La2) agree well with the value of 3.023 Å given in the literature for La^{3+} in an eightfold sulfur coordination (*17*). Figure 3 shows the lanthanum–sulfur arrangement

TABLE VIIA

$La_{32}Nb_{28}S_{88}$: INTERATOMIC DISTANCES (Å) FOR EACH POLYHEDRON

Within the "NbS_2" slab

Nb1–S2a	2.587(7)	Nb3–S4a	2.480(4)
S2b	2.587(7)	S4b	2.488(4)
S2c	2.579(8)	S1a	2.420(3)
S2d	2.457(7)	S1b	2.422(3)
S4a	2.622(5)	S3a	2.553(5)
S4b	2.548(4)	S3b	2.562(5)
Average	2.563	Average	2.487
Nb2–S2b	2.493(7)	Nb4–S1a	2.527(2)
S2c	2.353(8)	S1b	2.530(2)
S4a	2.480(5)	S3a	2.534(5)
S4b	2.398(4)	S3b	2.534(5)
S1a	2.633(4)	S1a	2.530(2)
S1b	2.558(4)	S1b	2.527(2)
Average	2.485	Average	2.530

For instance, the average (Nb–S) distance for NbS_3 is 2.54 (Ref. (*2*))

Within the "La–S" ladder

La1–S2a	2.850 (7)	La2–S1	2.930 (2)
S2b	3.631 (8)	S3	3.010 (5)
S4	3.040 (4)	S4	3.418 (3)
S5	2.772(12)	S5a	3.020 (5)
S6a	2.862(4)	S5b	2.954 (5)
S6b	2.950(8)	S5c	2.957 (5)
S6c	2.969(8)	S5d	2.929(10)
S6d	3.254(8)	S6	2.876 (6)
Average	3.041	Average	3.010

For instance, La–S distances (Å) given in the literature (*4*)

	$n = 6$	$n = 8$
La^{3+}	2.970	3.025

TABLE VIIB

INTERATOMIC DISTANCES (Å) BETWEEN METAL ATOMS

Nb1 (z = 0.58)–Nb2 (z = 0.07)	3.287(6)
(z = 1.07)	3.291(6)
Nb2 (z = 0.08)–Nb3 (z = 0.57)	3.512(4)
(z = −0.42)	3.519(4)
Nb3 (z = 0.58)–Nb4 (z = 0.08)	3.330(3)
(z = 1.08)	3.324(3)
Nb1 (z = 0.58)–Nb1 (z = 0.08)	3.181(2)
(z = 1.08)	3.181(2)
Average	3.328

Shortest La–La distances

La1–La1	4.315(8)
La1–La2	3.980(4)
La2–La2	3.928(2)

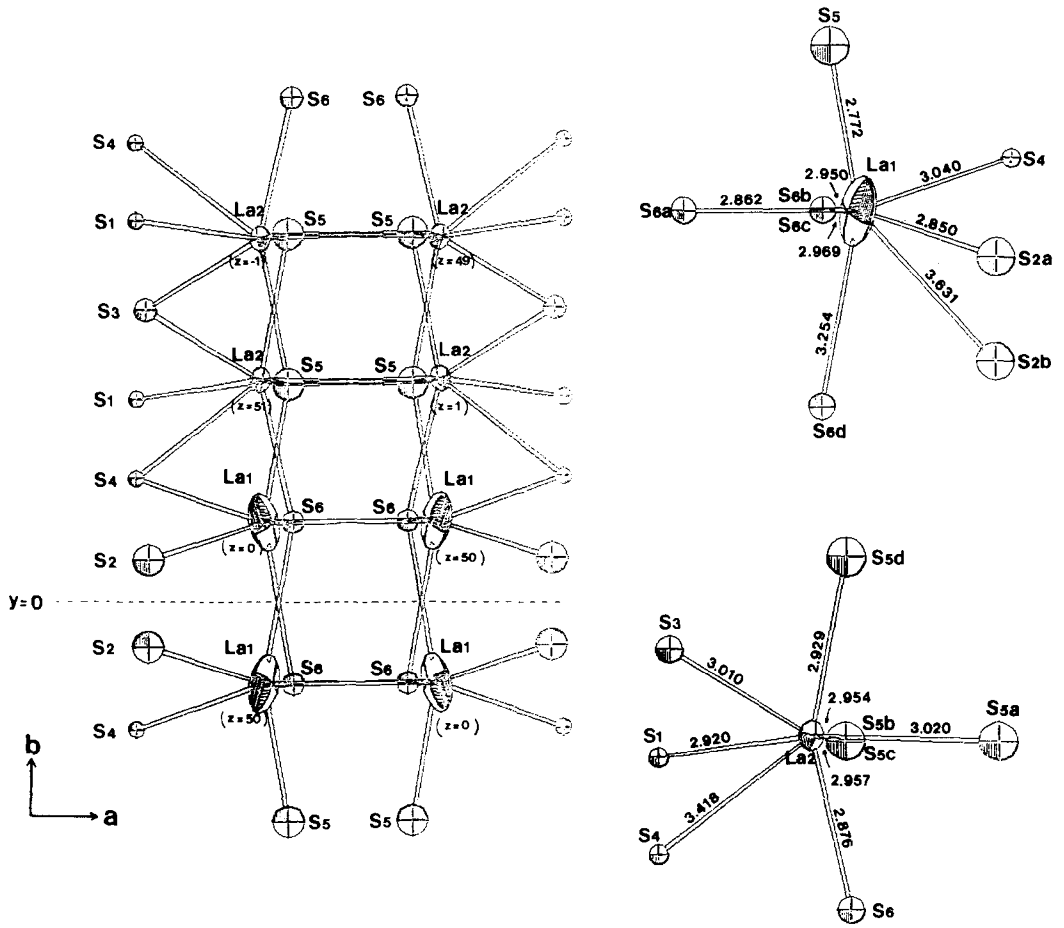

FIG. 3. "La–S" ladder arrangement and sulfur polyhedra around La1 and La2.

in the La–S layers, along with the La1 and La2 surroundings.

Discussion

The structure of $La_{32}Nb_{28}S_{88}$ recalls that of $La_{72}Cr_{60}S_{192}$ (commonly mentioned as "$LaCrS_3$") (*18a, 18b*). This latter phase was earlier described as consisting of alternating layers of |LaS| and $|CrS_2|$ parallel to (001). The $|CrS_2|$ layers have a CdI_2-like organization while the |LaS| layer exhibits a NaCl-like atomic arrangement. A schematic representation is shown in Fig. 4. But things are a bit more complicated and that structure has been thoroughly discussed in terms of order–disorder (OD) in connection with a lack of commensurability between both kinds of layers. Moreover, that structure was determined on the basis of a twinned crystal data. The unit cell parameters of an individual twin were found equal to:

$$\begin{aligned} a &= 5.94\ \text{Å} & \alpha &= 90.3^\circ \\ b &= 17.2\ \text{Å} & \beta &= 95.3^\circ \\ c &= 66.2\ \text{Å} & \gamma &= 90.0^\circ \end{aligned}$$

The periodicity of alternated layers is $c/6$ (11.03 Å); in $La_{32}Nb_{28}S_{88}$ it is expressed by $a/2$ (11.52 Å). The difference in thickness

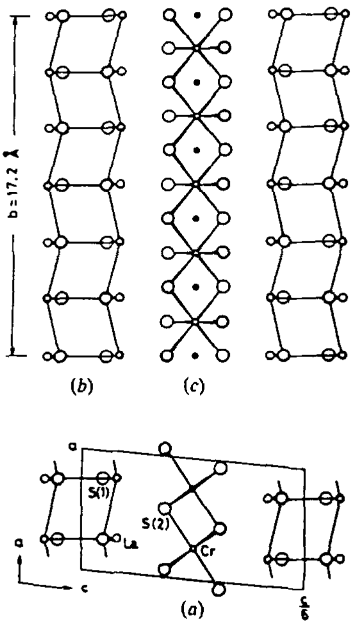

FIG. 4. Schematization of the "LaCrS$_3$" structural type (after (*18a*)).

can be of course related to the difference of size of chromium and niobium, but it also expresses the usual difference of thickness of an |MS_6| trigonal antiprismatic (CrS_6-octahedral) as compared to an |MS_6| trigonal prismatic (NbS_6) coordination in a layer structure (compare, for example, [NaS_6] in both cases in Na_xTiS_2 derivatives (*19*)).

In the case of "LaCrS$_3$," the |CrS_2| layers are stacked with vector $-b/30 + c/6$ (Fig. 5). There is no clear evidence of such a complicated stacking order in $La_{32}Nb_{28}S_{88}$.

In the course of the structural refinement we were led to assume a half-occupancy of Nb sites since the closest generated positions could be filled at the same time (too short Nb–Nb contacts, ≤ 2 Å). Thus, the half occupancy can reflect a situation where when one position is occupied the other one should be empty. This hardly suggests a kind of mismatch situation like in "LaCrS$_3$" (*18a, 18b*). Indeed, it is not to be excluded that the studied crystal was containing microdomains with some niobium atoms at z elevations such as 0.58 and 0.08, and some others at 0.92 and 0.42. What we took into consideration was an equal probability of 50–50% for such different domains. This is imposed by the *Ccca* space group and corresponds to an average solution of a likely more complex situation. In that way, a better solution could perhaps be obtained by decorrelating the occupancy of these two closest positions (through a change of space group) and then refining X and $1 - X$, respectively. However, this is neither a cer-

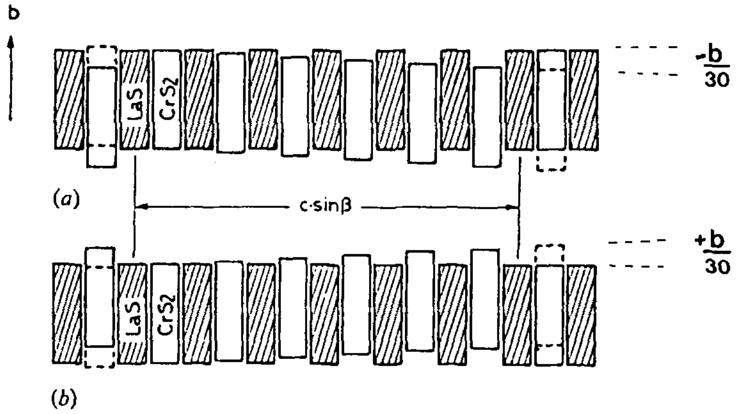

FIG. 5. Mismatch of alternated layers of |LaS| and |CrS_2| along the c axis.

TABLE VIII

STATISTICS BASED ON *hkl* INDICES ACCORDING TO *k* VALUES (21 FIRST VALUES)

K	No. of *hkl*	F_{obs} average	*R*	R_w
-0	58	536	-0.162	0.188
1	27	91	0.143	0.183
2	2	47	0.263	0.265
3	25	102	0.167	0.200
*4	42	390	*0.063	0.074
5	20	87	0.195	0.230
6	16	56	0.477	0.525
-7	46	416	-0.259	0.305
*8	57	365	*0.069	0.070
9	16	73	0.269	0.312
10	8	70	0.491	0.562
11	21	95	0.215	0.244
*12	38	324	*0.035	0.041
13	7	61	0.336	0.393
-14	50	351	-0.236	0.263
15	21	84	0.171	0.214
*16	45	276	*0.099	0.113
17	0	—	—	—
18	7	74	0.389	0.443
19	9	87	0.133	0.150
*20	24	230	*0.064	0.070
-21	29	270	-0.285	0.332

Note. * mod. 4. — mod. 7.

tainty nor an obvious solution, although the structure is well established in other respects.

A detailed analysis of the *R* factor shows inhomogeneous results according to the *hkl* data groups. Particularly, if one classifies *hkl* reflections as *h0l*, *h1l*, *h2l*, *h3l* . . . , the *R* values range between 0.03 and 0.49 (see Table VIII). One can also notice that intensities of some reflections are much larger when hkl indices are concerned with *k* values of type:

—k = 4, 8, 12 . . . mod. 4, in relation with the "La–S sublattice" which exhibits a periodicity of 4|La–S| small bars along the *b* axis;

—k = 0, 7, 14 . . . mod. 7, in connection with the "NbS_2 sublattice" which exhibits a periodicity of 7|NbS_2| also along the *b* axis.

In addition, the *R* values are markedly lower for *hkl* reflections with $k = 0$ mod. 4 group than for those belonging to the $k = 0$ mod. 7 group. This corresponds to the fact that the complications met in the structural determination are to be associated with the "NbS_2 sublattice." A similar presentation has been done for "$LaCrS_3$." Thus, *R* factors calculated for *hkl* reflections with $k = 0$ mod. 3 (La–S sublattice) are much lower than those calculated when $k = 0$ mod. 5 (CrS_2 sublattice). *R* factor values increase when F_{obs} values decrease.

Another factor attached to the relative periodicities of both |LaS| and |NbS_2| layers could have prevented the *R* factor to decrease. The unit cell as deduced from least-squares refinement of a powder pattern leads to a *b* parameter of 23.181 Å which corresponds to 7|NbS_2| for 4|LaS| entities along the *b* direction. A commensurate situation has been considered. The situation was found to be somewhat different for "$LaCrS_3$" and "$SnNbS_3$" as both compounds are illustrative of misfit layer structures. For "$LaCrS_3$," the structure determination was done with a 5/3 ratio along the layer (5|CrS_2| for 3|LaS| entities) but an electron diffraction study (*18a, 18b*) gave evidence of a mismatch in the *b* direction between subcells of the two layers types. Wiegers *et al.* (*20*) have very recently reported similar features on "$SnNbS_3$"; an incommensurate ratio of 1.7081(5) is found between both layer types (|SnS| and |NbS_2|) which could be approximated as 17/10 or 12/7. An incommensurate situation which has to be resolved using a superspace symmetry is not to be completely excluded in "$LaNbS_3$" despite the fact that one did not find yet any clear evidence of it.

Beyond these remarks, the structural type is well established. Thus, we also ascertained the structure by calculating the

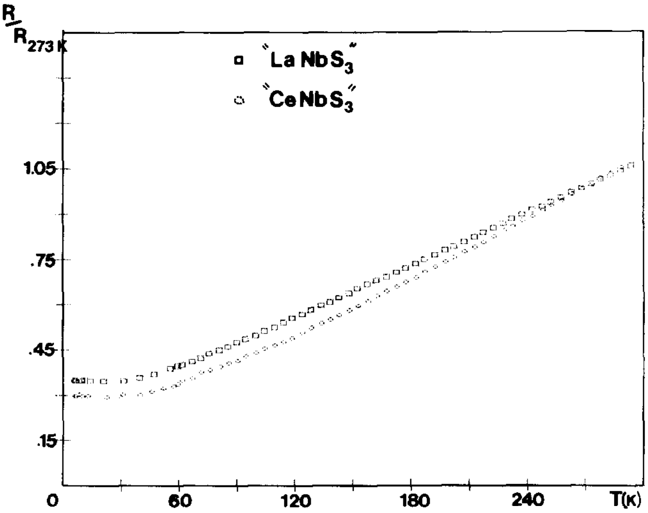

FIG. 6. Normalized resistance of "$LaNbS_3$" and "$CeNbS_3$" as a function of temperature.

relative intensities of the powder pattern with the LAZY-PULVERIX program (*21*) using the fractional coordinates obtained from the single-crystal determination. A good agreement is observed as only reflections appearing with significant calculated values, and all of them were indeed taken into account, which tends to prove the correctness of the proposed structure.

Conclusions

It can be said that $La_{32}Nb_{28}S_{88}$ represents a trigonal prismatic transposition of the "$LaCrS_3$" structural type. It shows alternatively trigonal prismatic $|NbS_2|$ layers separated by a $|LaS|$ region with a NaCl-like arrangement whereas "$LaCrS_3$" is built up from octahedral CdI_2-like $|CrS_2|$ slabs separated by similar $|LaS|$ domains.

The metallic behavior (Fig. 6) could come from the $|NbS_2|$ layers. However a comparison with tetrachalcogenides such as $(NbSe_4)_nI$ phases shows that a Nb–Nb distance of 3.51 Å is very likely too high to allow an electronic delocalization (*3*). Nevertheless the $|La–S|$ layer recalls that of the rare-earth monochalcogenides. They have the NaCl structure. LaS and CeS are metallic, their behavior being consistent with the formulation $La^{3+}(S^{2-})e^-$ (*22*). The same behavior holds for the reduced iodides LaI_2, CeI_2 according to the scheme $La^{3+}(I^-)_2e^-$ (*23*). It is likely that this situation is reproduced here and contributes largely, or even totally, to the metallic conductivity.

A series of phases, "$PbNbS_3$," "$PbTiS_3$," and "$SnTiS_3$," was recently synthesized and characterized through their unit cell parameters in a first approach (*12, 13, 24*). It appears clearly that these phases are directly related to $La_{32}Nb_{28}S_{88}$ and $La_{72}Cr_{60}S_{192}$. One expects a trigonal prismatic $|NbS_2|$ slab in "$PbNbS_3$" which would give the $Pb_{32}Nb_{28}S_{88}$ formulation and an octahedral $|TiS_2|$ slab in "$PbTiS_3$" and "$SnTiS_3$" with a connection with the "$LaCrS_3$" structural type.

Acknowledgments

We thank Dr. M. Guittard and Pr. J. Flahaut for providing us binary La_2S_3 and Ce_2S_3 samples. The authors are grateful to Dr. O. Peña and Pr. Sergent for fruitful discussions. We thank Pr. Wiegers *et al.* for sending their manuscript on $(SnS)_{1.18}NbS_2$, "SnNb S_3," prior to publication (*20*). This work was partly supported by NATO Grant 860438.

References

1. A. Meerschaut and J. Rouxel, *J. Less-Common Met.* **39,** 197 (1975).
2. J. Rijnsdorp and F. Jellinek, *J. Solid State Chem.* **25,** 325 (1978).
3. P. Gressier, A. Meerschaut, L. Guemas, J. Rouxel, and P. Monceau, *J. Solid State Chem.* **51,** 141 (1984).
4. P. Monceau (Ed.), "Electronic Properties of Inorganic Quasi ID Compounds," Reidel, Dordrecht (1985).
5. S. J. Hillenius, R. V. Coleman, R. M. Fleming, and R. J. Cava, *Phys. Rev. B* **23,** 1567 (1981); R. J. Cava, V. L. Himes, A. D. Mighell, and R. S. Roth, *Phys. Rev. B* **24,** 3634 (1981); A. Meerschaut, P. Gressier, L. Guemas, and J. Rouxel, *Mater. Res. Bull.* **16,** 1035 (1981).
6. S. A. Sunshine and J. A. Ibers, *Inorg. Chem.* **24,** 3611 (1985).
7. S. A. Sunshine and J. A. Ibers, *Inorg. Chem.* **25,** 4355 (1986).
8. F. Jellinek, *Mater. Res. Bull.* **6,** 169 (1971).
9. G. V. Subba Rao, M. W. Shafer, and L. J. Tao, *Mater. Res. Bull.* **8,** 1231 (1973).
10. Kazuya Suzuki, Norimichi Kojima, Toshiro Ban, and Ikuji Tsujikawa, *Synth. Met.* **19,** 893 (1987).
11. P. C. Donohue, *J. Solid State Chem.* **12,** 80 (1975).
12. L. Schmidt, *Phys. Lett. A* **31**(10), 551 (1970).
13. M. H. Van Maaren, *Phys. Lett. A* **40**(5), 353 (1972).
14. T. Okabe, G. Van Tendeloo, J. Van Landuyt, S. Amelinckx, and M. Guittard, *J. Solid State Chem.* **72**(2), 376 (1988).
15. Vo Van Tien, M. Guittard, J. Dugue, and J. Flahaut, *J. Solid State Chem.* **73**(1), 11 (1988).
16. B. Frenz, "Enraf–Nonius Structure Determination Package," Delft Univ. Press, Delft (1982).
17. P. Poix, *C.R. Acad. Sci. Paris* **270,** 1852 (1970).
18a. Katsuo Kato, Isao Kawado, and Tatsuo Takahashi, *Acta Crystallogr. Sect. B* **33,** 3437 (1977).
18b. L. Otero-Diaz, J. D. Fitzgerald, T. B. Williams, and B. G. Hyde, *Acta Crystallogr. Sect. B* **41,** 405 (1985).
19. P. Molinie, L. Trichet, J. Rouxel, C. Berthier, Y. Chabre, and P. Segransan, *J. Phys. Chem. Solids* **451,** 105 (1984).
20. G. A. Wiegers, A. Meetsma, R. J. Haange, and J. L. de Boer, *Mater. Res. Bull.*, preprint.
21. R. Yvon, W. Jeitschko, and E. Parthe, *J. Appl. Crystallogr.* **10,** 73 (1977).
22. J. Flahaut, *in* "Handbook on the Physics and Chemistry of Rare Earths" (K. A. Gschneider, Jr. and L. Eyring, Eds.), Vol. 4, p. 17, Elsevier, Amsterdam/New York (1979).
23. M. Haschke, *in* "Handbook on the Physics and Chemistry of Rare Earths" (K. A. Gschneider, Jr. and L. Eyring, Eds.), Vol. 4, p. 114, Elsevier, Amsterdam/New York (1979).
24. L. Guemas, P. Rabu, A. Meerschaut, and J. Rouxel, *Mater. Res. Bull.* **23,** 7 (1988).